Anelastic Relaxations of La-based Amorphous Alloys

Anelastic Relaxations of La-based Amorphous Alloys*

Hiroshi Okumura**, Akihisa Inoue and Tsuyoshi Masumoto

Institute for Materials Research

(Received January 31, 1992)

Synopsis

The relaxation processes of La-based amorphous alloys with distinct glass transition phenomenon have been investigated in the temperature regions around the glass transition temperature and well below the glass transition temperature by the dynamic mechanical measurements. The amorphous alloys used in this study are $La_{55}Al_{45-x}Ni_x$ (x=0 to 35 %) and $La_5Al_{85}Ni_{10}$ alloys for examination of the compositional effect and $La_{55}Al_{25}M_{20}$ (M=Cu, Pd or Au) alloys for the substitutional effect. The sub-T_g relaxation phenomenon was observed for $La_{55}Al_{45-x}Ni_x$ (x=5 to 35 %) and $La_5Al_{85}Ni_{10}$ amorphous alloys. The relaxation due to the glass transition was recognized for $La_{55}Al_{45-x}Ni_x$ (x=0 to 35 %), $La_5Al_{85}Ni_{10}$ and $La_{55}Al_{25}M_{20}$ (M=Cu, Pd or Au) amorphous alloys. In addition, the second-stage relaxation in the glass transition region was also observed for $La_{55}Al_{45-x}Ni_x$ (x=15 to 30 %) and $La_{55}Al_{25}M_{20}$ (M=Cu, Pd or Au) amorphous alloys with a wide supercooled liquid region exceeding 35 K. The appearance of the two kinds of relaxation units seems to reflect the difference in the chemical bonding nature among the constituent elements.

I. Introduction

It is well known that oxide and fluoride glasses exhibit a wide supercooled liquid region before crystallization and their glassy structure has high stability against crystallization in the supercooled liquid region. On the other hand, no glass transition phenomenon has been observed in a majority of metallic amorphous alloys.

---

* The 1878th report of Institute for Materials Research.

** Graduate student, Tohoku University.

The appearance of a wide supercooled liquid region before crystallization had been limited to Pt- and Pd-based amorphous alloys[1]. Recently, Inoue et al. have reported[2,3] that La-, Zr- and Mg-based amorphous alloys exhibit a wide supercooled liquid region comparable to that for Pt-Ni-P amorphous alloys. Consequently, the use of these new amorphous alloys is expected to shed some light on clarification of an inherent nature of the glass transition in amorphous alloys. The information on the glass transition appears to be essential for scientific and technological progresses of the new-type amorphous alloys. Since the glass transition is a dynamical transition, the increase of relaxation time caused by the progress of structural relaxation in the glass transition region causes the significant changes in viscosity, diffusivity, specific heat and so forth[4] for an amorphous solid. When an amorphous alloy is heated, a frozen atomic configuration is cooperatively released at the glass transition temperature[5], accompanying the increase in the degree of anelasticity for an elastic amorphous solid. We have already reported that a $La_{55}Al_{25}Ni_{20}$ amorphous alloy with the widest supercooled liquid region in the La-Al-Ni system shows the two-stage relaxation phenomenon in the glass transition region[6] and the sub-T_g relaxation at temperatures well below the glass transition temperature[7,8] by dynamic mechanical measurements. This paper is intend to examine the compositional effect on the sub-T_g and two-stage relaxation phenomena of La-Al-Ni and La-Al-M (M=Cu, Pd or Au) amorphous alloys.

II. Experimental Procedure

Binary La-Al and ternary La-Al-M (M=Ni, Cu, Pd or Au) alloys were used in the present study. Their ingots were prepared by arc melting a mixture of pure (99.9 mass %) La, Al, Ni, Cu, Pd and Au metals in a purified argon atmosphere. The compositions are nominally expressed in atomic per cent. From the master alloy ingots, ribbons with a cross section of about 0.03x1 mm^2 were prepared by a single roller melt-spinning technique in an argon atmosphere. The amorphous state of the ribbons was examined by X-ray diffractometry. The apparent specific heat (C_p) associated with structural relaxation, glass transition and crystallization was measured with a differential scanning calorimeter (DSC) at a heating rate of 0.67 K/s. Temperature- and frequency-dependent dynamic mechanical properties of storage (E') and loss (E") moduli were measured by a forced oscillation method (Rheometrics RSA-II). Detailed procedures were described

in refs. 6 to 9.

III. Results and Discussion

1. Compositional effect on relaxations of La-Al-Ni amorphous alloys

As reported previously[2], the composition range in which an amorphous La-Al-Ni phase is formed by melt spinning is quite wide and can be divided into two categories of La-rich and Al-rich compositions; 0 to 55 %Al and 0 to 60 %Ni for the La-rich alloys and 70 to 90 %Al and 0 to 15 %Ni for the Al-rich alloys. In this section, $La_{55}Al_{45-x}Ni_x$ (x=0 to 35 %) and $La_5Al_{85}Ni_{10}$ are chosen as the La-rich and Al-rich alloys, respectively, for the examination of the compositional effect.

Figure 1 shows the DSC curves of the $La_{55}Al_{45-x}Ni_x$ and $La_5Al_{85}Ni_{10}$ alloys. It is seen that the $La_{55}Al_{45}$ alloy crystallizes through a single stage at a heating rate of 0.67 K/s and the onset temperature of crystallization (T_x) is indicated by upward arrows. The ternary alloys have more complex crystallization processes. That

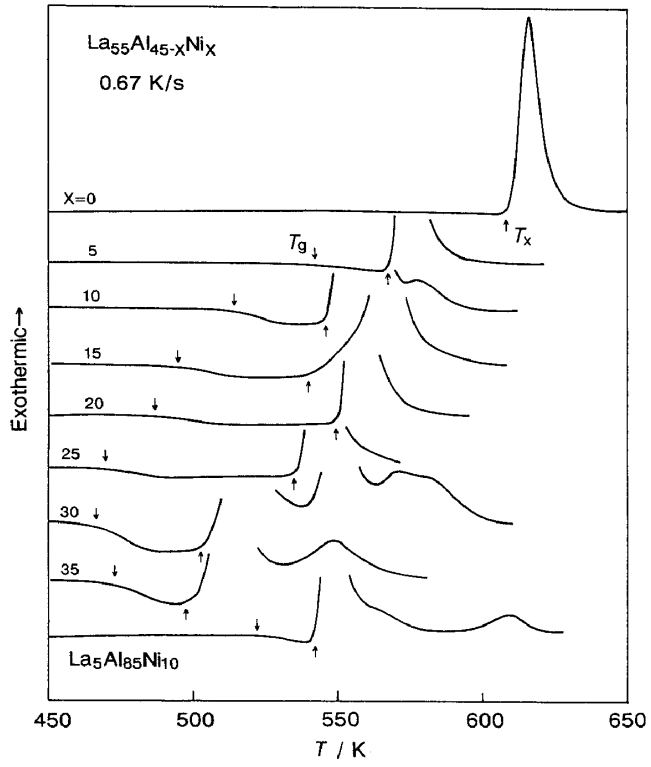

Fig. 1 Differential scanning calorimetric curves of $La_{55}Al_{45-x}Ni_x$ (x=0 to 35 at%) and $La_5Al_{85}Ni_{10}$ amorphous alloys.

is, the alloys with x=10, 30 and 35 % have a few exothermic peaks while those with x=20 and 25 % show only one peak. In the case of x=15 %, only one peak is seen, but its onset point is not clear as that for the other alloys and the peak appears to separate at lower heating rates. The $La_5Al_{85}Ni_{10}$ alloy also shows a few endothermic peaks. Although no distinct endothermic reaction below T_x is seen for the $La_{55}Al_{45}$ alloy, the addition of Ni causes an endothermic reaction due to glass transition as indicated by downward arrows. The temperature span of the supercooled liquid region ($\Delta T_x=T_x-T_g$) increases with increasing Ni content from 5 to 20 % and decreases with a further increase in Ni content. To obtain further detailed information on the glass transition, the temperature dependence of specific heat (C_p) for these alloys has been measured and the results are shown in Fig. 2. The samples are first heated to the temperature of the supercooled liquid to obtain the data in the as-quenched state ($C_{p,q}$, broken lines), and then cooled to room temperature. The measurement is immediately repeated in situ to obtain the data of the reference sample ($C_{p,s}$, solid lines). The heating- and cooling-rates are kept at 0.67 K/s. The $C_{p,s}$ curve is independent of thermal history and consists of configurational contribution as well as that arising from purely thermal vibrations. The difference in $C_p(T)$ between the as-quenched state and the reheated states manifests the irreversible structural relaxation which is presumed to arise from the annihilation of various kinds of quenched-in defects and the enhancement of the topological and chemical short-range ordering through the atomic rearrangement. T_g and T_x are defined as the points of intersection of two tangent lines at the endothermic and exothermic peaks, respectively, on the $C_{p,s}$ curve. For instance, T_g, T_x and ΔT_x for the x=20 % alloy are 481, 546 and 65 K, respectively. It is seen that $C_{p,s}$ increases rapidly at T_g and shows an equilibrium specific heat of the supercooled liquid as a plateau. The increase in the specific heat caused by the glass transition reaches 12 J/(molK). $C_{p,s}$ of the x=0 alloy increases slightly at about 590 K, followed by crystallization. The slight increase is also thought to correspond to the initial stage of the glass transition.

Figure 3 shows T_g, T_x and ΔT_x obtained from the $C_{p,s}$ data for the $La_{55}Al_{45-x}Ni_x$ and $La_5Al_{85}Ni_{10}$ amorphous alloys. T_g decreases from 539 to 462 K with increasing x content from 5 to 30 % and then increases slightly at x=35 %. T_x also tends to decrease with increasing x content, though a slight increase is seen at x=20 %. The increase in T_x around x=20 % causes larger ΔT_x values. As men-

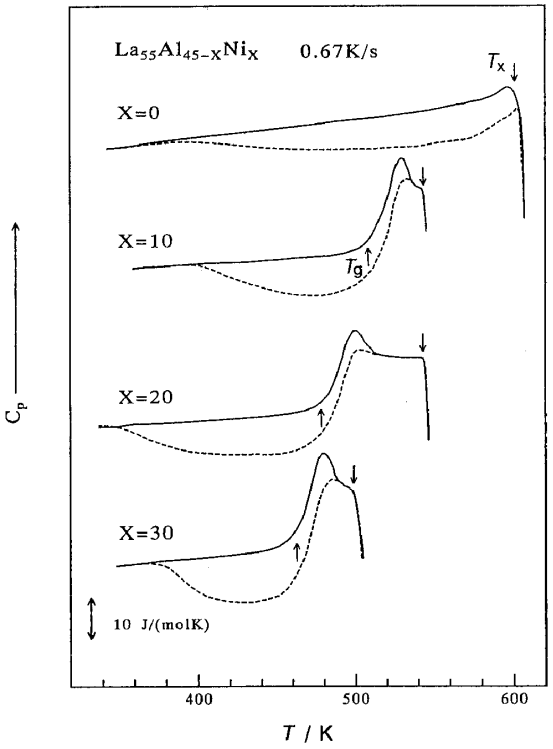

Fig. 2 The thermograms $C_{p,q}(T)$ of $La_{55}Al_{45-x}Ni_x$ (x=0, 10, 20 and 30 %) amorphous alloys. The solid lines represent the thermograms $C_{p,s}$ of the samples once heated up to T_g.

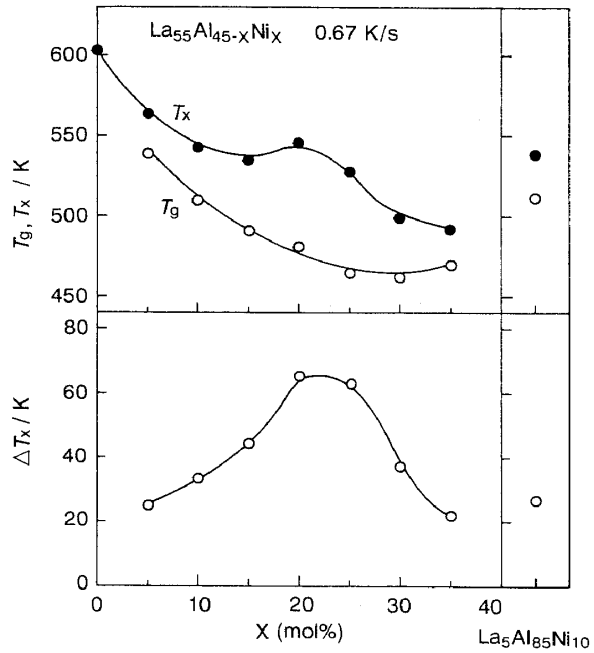

Fig. 3 T_g, T_x and ΔT_x for $La_{55}Al_{45-x}Ni_x$ (x=0 to 35 %) and $La_5Al_{85}Ni_{10}$ amorphous alloys.

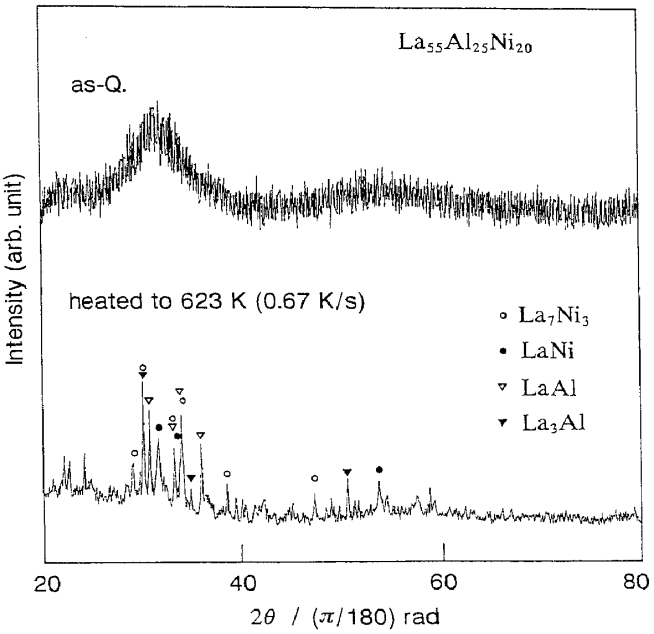

Fig. 4 X-ray diffraction patterns of a $La_{55}Al_{25}Ni_{20}$ amorphous alloy in as-quenched and fully crystallized states.

tioned before, a single crystallization peak appears in the vicinity of the composition with ΔT_x over 60 K, suggesting that the crystallization process changes around the composition (Al/Ni≈1). The initial stage in the crystallization process is thought to be affected by equilibrium Al-La binary phases for the Al-rich alloys and by the equilibrium Ni-La phases for the Ni-rich alloy. The X-ray diffraction patterns of the x=20 % alloy shown in Fig. 4 indicate that binary intermetallic compounds of La_7Ni_3, LaNi, LaAl and La_3Al precipitate after the single crystallization peak. The long-range rearrangement of the constituent elements is required for the simultaneous precipitation of these compounds. Al and Ni atoms must be removed to form the La-Ni and La-Al binary compounds and the difficulty of long-range diffusion for this elements results in an increase in T_x leading to the increase in ΔT_x with the largest value around Al/Ni≈1. T_g and T_x of the $La_5Al_{85}Ni_{10}$ amorphous alloy are 512 and 539 K, respectively, being similar to those for the $La_{55}Al_{35}Ni_{10}$ alloy with a lower Ni concentration.

The temperature dependence of E' and E" for $La_{55}Al_{45-x}Ni_x$ and $La_5Al_{85}Ni_{10}$ amorphous alloys was measured to detect relaxation processes. The measurements were made at a heating rate of 0.083 K/s and at frequencies (ω) of 62.8, 6.28 and 0.628 rad/s. Figures 5 and 6 show the data on E' and E" at 6.28 rad/s, respectively. With in-

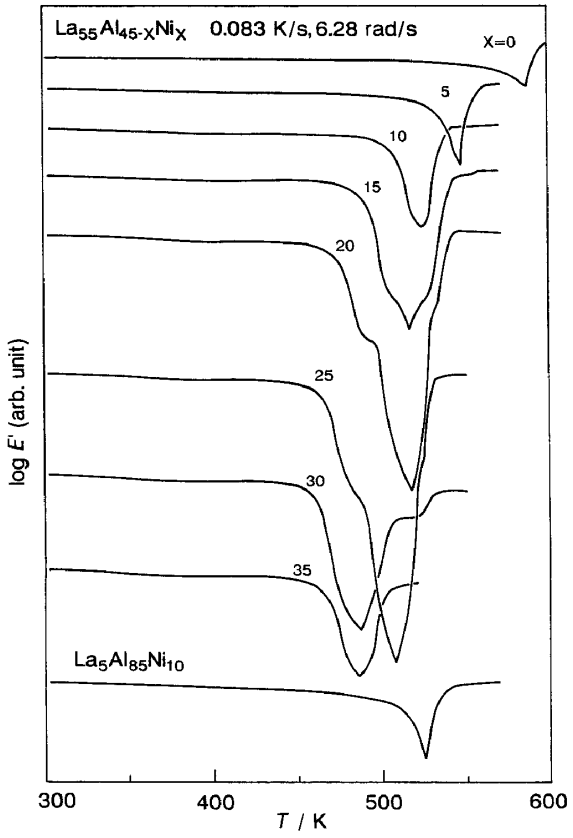

Fig. 5
Temperature dependence of E' at 6.28 rad/s for $La_{55}Al_{45-x}Ni_x$ (x=0 to 35 %) and $La_5Al_{85}Ni_{10}$ amorphous alloys.

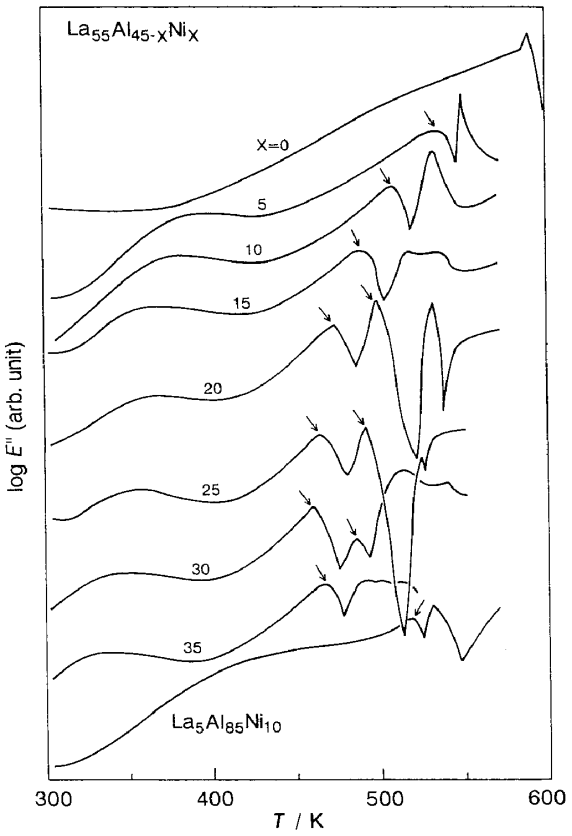

Fig. 6
Temperature dependence of E" at 6.28 rad/s for $La_{55}Al_{45-x}Ni_x$ (x=0 to 35 %) and $La_5Al_{85}Ni_{10}$ amorphous alloys.

creasing temperature, E' decreases slightly in the amorphous solid region and rapidly in the glass transition region and then increases due to crystallization. It is seen in Fig. 5 that E' for the x=0 alloy begins to decrease at about 575 K and increases at 587 K. The decrease of E' is smaller as compared with the ternary alloys exhibiting distinct T_g on the DSC curves. One can see a tendency that the larger the ΔT_x value, the larger is the decrease in E'(T). When the x content increases to 15 %, the two-stage reduction of E'(T) is seen at each onset temperature of 483 and 507 K. The two-stage reduction indicates that the $La_{55}Al_{30}Ni_{15}$ alloy has two kinds of relaxation units in the glass transition region[6]. The increase in ΔT_x results in an appearance of more distinct second-stage reduction of E'(T). The temperature span at the second-stage is about 10 K for the x=15 alloy and 30 K for the X=20 alloy, in contrast to the result that at the first-stage is about 25 K for the former alloy

and 20 K for the latter alloy. The difference suggests that the second-stage reduction of E' has a close relation with ΔT_x. The composition range in which the two-stage reduction phenomenon is observed is in the x range of 15 to 25 % at a frequency of 6.28 rad/s. The further increase in x above 30 % causes the disappearance of the second-stage reduction of E' as well as the smaller decrease in E', accompanying the decrease in ΔT_x.

Figure 6 shows the temperature dependence of E" for the $La_{55}Al_{45-x}Ni_x$ and $La_5Al_{85}Ni_{10}$ amorphous alloys. E" of the x=0 alloy shows only a crystallization peak at 589 K. For the x=5 alloy with distinct T_g, a peak due to the glass transition is observed at 536 K before a crystallization peak at 550 K. The peak at 536K was confirmed to be due to the relaxation process through the measurements at different frequencies. Only the peaks due to relaxation are indicated by arrows. For instance, E" of the x=15 alloy shows only one relaxation peak at 489 K, though the E'(T) curve at 6.28 rad/s shows distinct two-stage reduction resulting from two relaxation units. It has further been clarified from the measurement at different frequencies that the second-stage relaxation peak at 6.28 rad/s overlaps with a crystallization peak while that at 0.628 rad/s can be separated from the crystallization peak (cf. Fig. 7). As shown for the DSC curve in Fig. 1, the crystallization of this alloy occurs gradually and the onset of the exothermic peak is dull. This crystallization behavior appears to reflect the E"(T) behavior. Before the second-stage relaxation is completed, the crystallization starts and the difference in the relaxation times between the second-stage relaxation and the crystallization is too small to separate the E"(T) behavior at higher frequencies. This suggests that the stability of the supercooled liquid against the nucleation of a crystalline phase for this alloy is not so high as that expected from ΔT_x. On the other hand, the x=20, 25 and 30 alloys show distinct two-stage peaks even at this frequency.

Peak temperatures (T_p) of the relaxation peaks for $La_{55}Al_{45-x}Ni_x$ and $La_5Al_{85}Ni_{10}$ alloys measured at three frequencies are plotted as a function of x content in Fig. 7. It is thought that the increase in the stability against the nucleation of a crystalline phase in the supercooled liquid of an amorphous alloy causes a distinct appearance of the relaxation peak even in a high frequency range. The lack of the relaxation peak at 62.8 rad/s for the Al-rich $La_5Al_{85}Ni_{10}$ alloy indicates that the stability of the Al-rich alloy is lower as compared with the La-rich alloys with nearly the same ΔT_x values. This difference may result from the differences in the crystallization

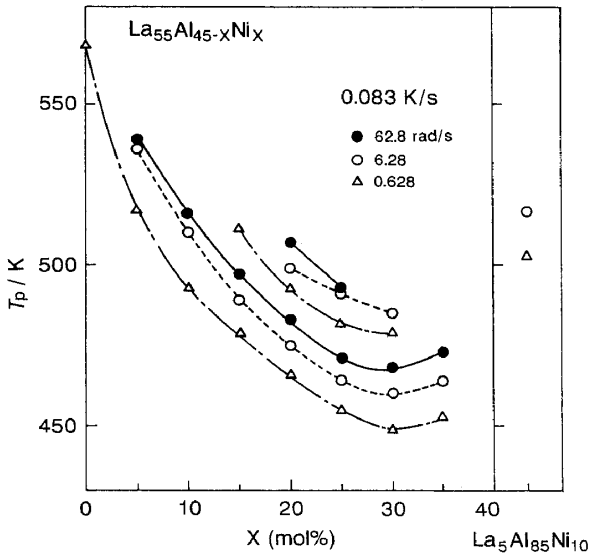

Fig. 7 The peak temperatures of the relaxation peaks in the glass transition region for $La_{55}Al_{45-x}Ni_x$ (x=0 to 35 %) and $La_5Al_{85}Ni_{10}$ amorphous alloys.

process and the bonding nature of the constituent atoms. The existence of a strong interaction between Al and Y in Al-Y-Ni alloys has been reported[10]. Figure 4 also suggests that a strong interaction of La-Al and La-Ni pairs exists in the La-Al-Ni system. The number of Al-Al pair is larger for the Al-rich alloys than for the La-rich alloys and the difference in the number of Al-Al pair seems to cause the difference in the stability of the supercooled liquid region between the Al-rich and the La-rich alloys with similar ΔT_x values. Moreover, the bonding nature also has a dominant effect on the sub-T_g peak[7,8] of E", as shown in Fig. 6. The sub-T_g peak for the $La_5Al_{85}Ni_{10}$ alloy appears to be broader at higher temperatures as compared with the La-rich alloys with a similar T_g and the discussion about the sub-T_g relaxation will be given later. The La-Al-Ni alloys with ΔT_x exceeding 35 K measured at 0.67 K/s have two-stage relaxation spectra, but the two-stage relaxation process cannot be observed on the DSC curves, as shown in Figs. 1 and 2. It should be noticed that the x=0 alloy without T_g shows a broad relaxation peak at 568 K in the case of 0.628 rad/s, indicating that a slight relaxation occurs in spite of the absence of T_g on the DSC curve. The difference seems to be attributed to the difference in the mechanism; the DSC data contains the static thermal transient behavior while the dynamic mechanical measurements contains the information from dynamic atomic movement.

2. $La_{55}Al_{25}Ni_{20}$ and $La_{55}Al_{35}Ni_{10}$ alloys

In this section, we chose a $La_{55}Al_{25}Ni_{20}$ with two-stage relaxation units at T_g and a $La_{55}Al_{35}Ni_{10}$ with one relaxation unit in order to examine the differences in the sub-T_g and T_g relaxation behaviors between both the alloys.

Figure 8 shows the isothermal frequency dependence of E' and E" for the $La_{55}Al_{35}Ni_{10}$ alloy in the temperature range where the sub-T_g relaxation occurs. The measurements were made six times for the same sample at a temperature interval of 20 K in the range of 353 to 453 K and the frequency was changed in the range of 10^{-1} to 10^{2} rad/s. The sample was once heated to 510 K to stabilize the structure. At 353 K, E' increases with increasing frequency while E" shows a peak for the sub-T_g relaxation at about 0.4 rad/s. With increasing temperature, the peak of E" increases gradually, accompanying the peak shift to a higher frequency side, while E' decreases gradually and the plateau of E' corresponding to the peak of E" also shifts to a higher frequency side. A drastic decrease in E' and an increase in E" at temperatures above 433 K are seen in the lower frequency region because of the approach to the glass transition. Figure 9 shows a master curve of E" for the sub-T_g relaxation at 373 K obtained by the time-temperature superposition process from the data shown in Fig. 8. The data at each temperature are shifted horizontally and vertically such that the E" peak coincides with the data at 373 K. The quantity of the shift, which is the ratio of the shifted frequencies set at 373 K (ω_0) to measured frequencies at each temperature (ω), is called as the shift factor ($a_\tau = \omega_0/\omega$) and the temperature dependence of a_τ gives the apparent activation energy for the relaxation. The overall E"($\log\omega$) thus obtained lies over the wide frequency range of about six orders which cannot be obtained only through one measurement, indicating clearly the existence of the sub-T_g relaxation peak at about 2 rad/s.

The secondary β-relaxation at temperatures well below T_g is usually seen in polymers and molecular glasses by mechanical and/or dielectric measurements[11]. The β-relaxation obeys the Arrhenius equation and ln a_τ can be expressed by a linear function of 1/T, though the α-relaxation of the glass transition does not obey the Arrhenius relation. Figure 10 shows the temperature dependence of the shift factor for the $La_{55}Al_{35}Ni_{10}$ alloy and the data obey the Arrhenius equation with a good linearity between ln a_τ and 1/T. The activation energy for this relaxation is evaluated to be 93 kJ/mol

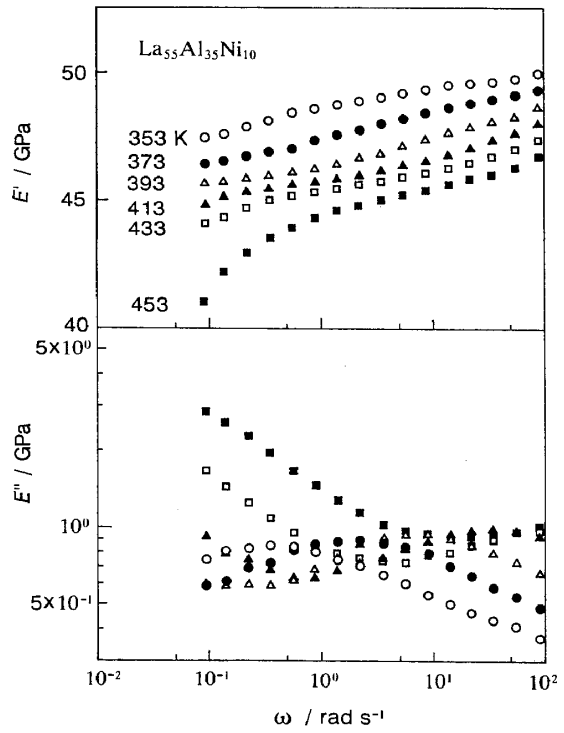

Fig. 8 Frequency dependence of E' and E" in the temperature region for the sub-T_g relaxation of a $La_{55}Al_{35}Ni_{10}$ amorphous alloy.

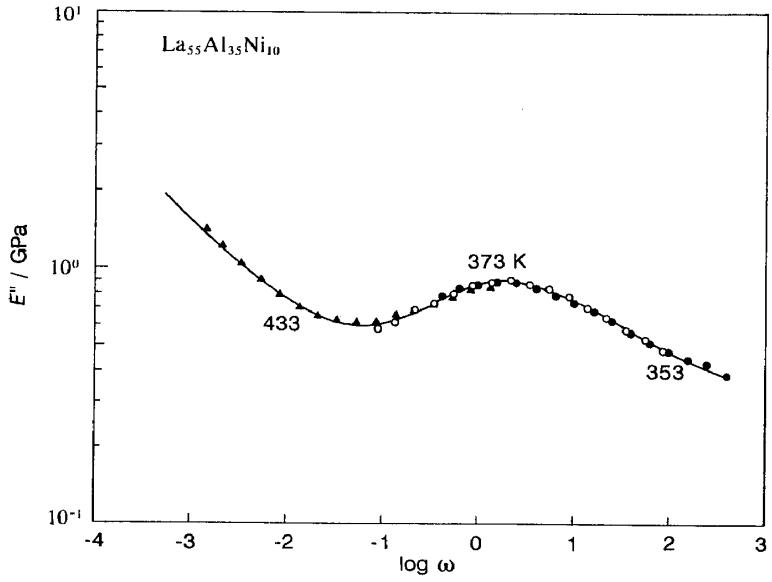

Fig. 9 Master curve of E"(log ω) at 373 K for the sub-T_g relaxation of a $La_{55}Al_{35}Ni_{10}$ amorphous alloy.

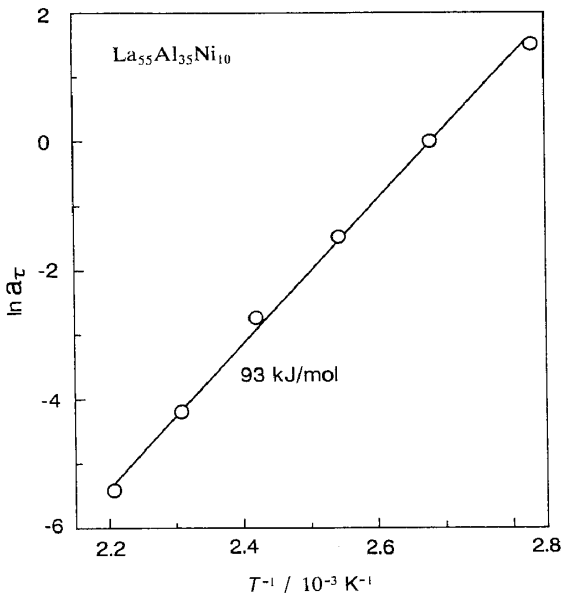

Fig. 10
Temperature dependence of a_τ for the sub-T_g relaxation of a $La_{55}Al_{35}Ni_{10}$ amorphous alloy.

from the gradient of the line. We previously reported the sub-T_g relaxation behavior for the $La_{55}Al_{25}Ni_{20}$ alloy[7,8]. The activation energy for the sub-T_g relaxation of the $La_{55}Al_{25}Ni_{20}$ alloy evaluated from E" is 97 kJ/mol which is nearly the same as that of the $La_{55}Al_{35}Ni_{10}$ alloy. All the ternary $La_{55}Al_{45-X}Ni_X$ amorphous alloys show the distinct sub-T_g relaxation while no sub-T_g relaxation peak is observed for the $La_{55}Al_{45}$ alloy without Ni, as shown in Fig. 6. The peak of the $La_5Al_{85}Ni_{10}$ alloy with a smaller Ni concentration is rather vague. The sub-T_g relaxation is independent of both the magnitude of ΔT_x and the relaxation units in the glass transition region and depends on the bonding nature among the constitutional atoms.

Figure 11 shows the temperature dependence of E' and E" in the glass transition region for the $La_{55}Al_{35}Ni_{10}$ alloy measured at different frequencies of 62.8, 6.28 and 0.628 rad/s. E' begins to decrease rapidly due to the glass transition at temperatures above 512 K in the case of 62.8 rad/s. The temperature at which E' begins to decrease shifts to a lower temperature side with decreasing frequency, e.g., 508 K at 6.28 rad/s and 493 K at 0.628 rad/s. However, the onset temperature for the rapid increase in E' caused by crystallization is 526 K and independent of frequency. On the other hand, E" shows a peak resulting from the relaxation of the glass transition and the peak temperature shifts to a lower temperature side from 516 to 493 K with decreasing frequency from 62.8 to 0.628 rad/s. The second-stage relaxation for the $La_{55}Al_{35}Ni_{10}$ alloy cannot be observed on the E'(T) and E"(T) curves even at the lowest frequency of 0.628 rad/s. Thus, one can notice the significant difference in the E'(T) and E"(T) behaviors between the $La_{55}Al_{35}Ni_{10}$ alloy with one peak and the $La_{55}Al_{25}Ni_{20}$ alloy with two peaks[6], as shown in Fig. 12. Two relaxation units in the glass transition region for the $La_{55}Al_{25}Ni_{20}$ alloy are clearly seen on the E'(T) and E"(T)

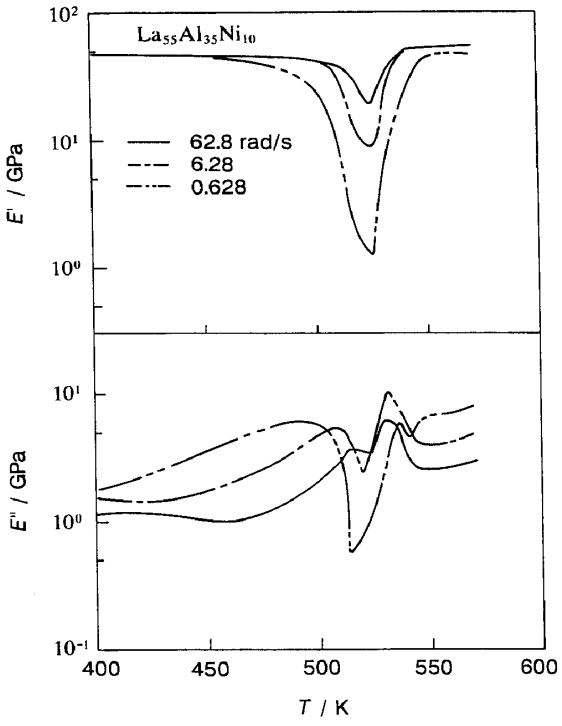

Fig. 11
Change in the temperature dependence of E' and E" for a $La_{55}Al_{35}Ni_{10}$ amorphous alloy.

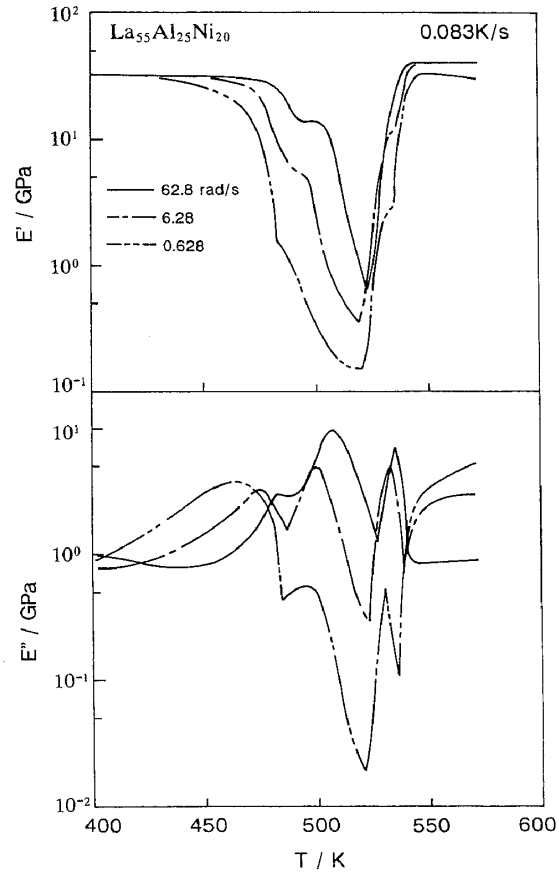

Fig. 12
Change in the temperature dependence of E' and E" for a $La_{55}Al_{25}Ni_{20}$ amorphous alloy.

curves. For instance, the first- and the second-stage of the reduction of E' occur at 479 and 491 K, respectively, and the two peaks of E" are observed at 483 and 507 K in the case of 62.8 rad/s.

Figure 13 shows the frequency dependence of E" in the glass temperature region for the $La_{55}Al_{35}Ni_{10}$ alloy. The peak is seen at temperatures above 488 K in the frequency range of 10^{-1} to 10^{2} rad/s and shifts to a higher frequency side with increasing temperature. The number of the points at temperatures above 508 K decreases because of the instability of the amorphous phase in the high temperature range. The E"(ω) data do not show any evidence of two relaxations. The peak value of about 10^{1} GPa is one order higher than that (about 10^{0} GPa) for the sub-T_g relaxation, indicating that the relaxation takes place more drastically as compared with the sub-T_g relaxation due to a short-range rearrangement. Figure 14

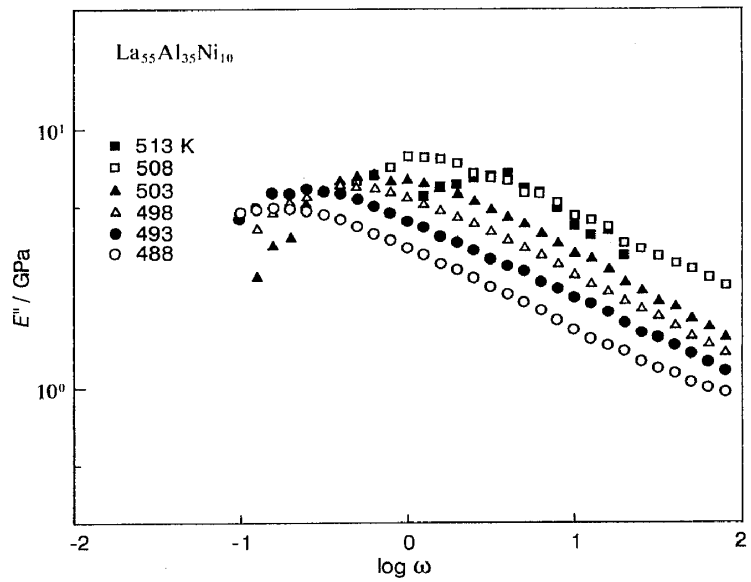

Fig. 13 Frequency dependence of E" in the glass transition region for a $La_{55}Al_{35}Ni_{10}$ amorphous alloy.

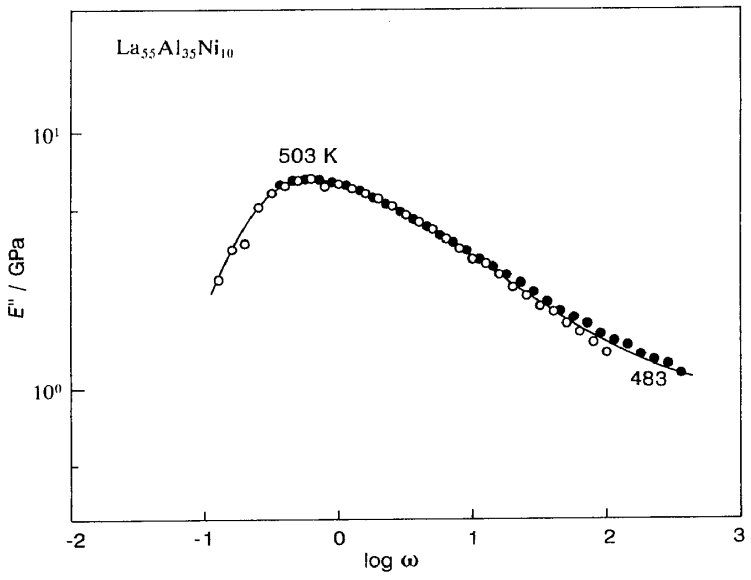

Fig. 14 Master curve of E"(log ω) at 503 K for a $La_{55}Al_{35}Ni_{10}$ amorphous alloy.

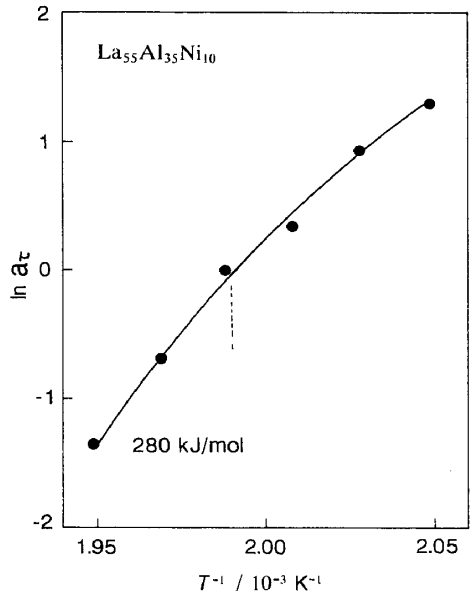

Fig. 15
Temperature dependence of a_τ for a $La_{55}Al_{35}Ni_{10}$ amorphous alloy.

shows the master curve of E" for the relaxation of the glass transition at 503 K which is derived by using the data shown in Fig. 13. Also, Fig. 15 shows the temperature dependence of a_τ. One can see a slight deflection at about 500 K in the relationship between ln a_τ and 1/T. The change in the slope suggests that the activation energy for the relaxation due to the glass transition increases with increasing temperature. The activation energy at temperatures above 503 K is evaluated to be 280 kJ/mol.

The activation energy (280 kJ/mol) is considerably smaller as compared with that for other amorphous alloys. That is, the activation energies for the first- and second-stage relaxations in the $La_{55}Al_{25}Ni_{20}$ alloy are 400 and 550 kJ/mol, respectively. The activation energies for the glass transition in Pd- and Pt-based amorphous alloys have been reported to be in the range from 400 to 750 kJ/mol[12] which roughly agrees with those for polymers[13]. The smaller activation energy of the $La_{55}Al_{35}Ni_{10}$ alloy seems to be attributed to the lower stability of the supercooled liquid. That is, crystallization begins to occur before the cooperative atomic rearrangement with higher activation energy. Figure 15 also suggests that the activation energy reaches as a high value of about 400 kJ/mol when the crystallization is suppressed and E"(ω) is measured at higher temperatures. As shown in Figs. 11 and 12, the decrease in E"(T) after the peak of the glass transition for the $La_{55}Al_{35}Ni_{10}$ alloy is smaller than that for the $La_{55}Al_{25}Ni_{20}$ alloy. This difference indicates that the supercooled liquid just before crystallization is in a more viscous flow state for the $La_{55}Al_{25}Ni_{20}$ alloy.

3. $La_{55}Al_{25}M_{20}$ (M=Cu, Pd or Au) alloys

It has previously been reported that an amorphous $La_{55}Al_{25}Cu_{20}$ alloy also shows a wide supercooled liquid region[3]. Also, the data

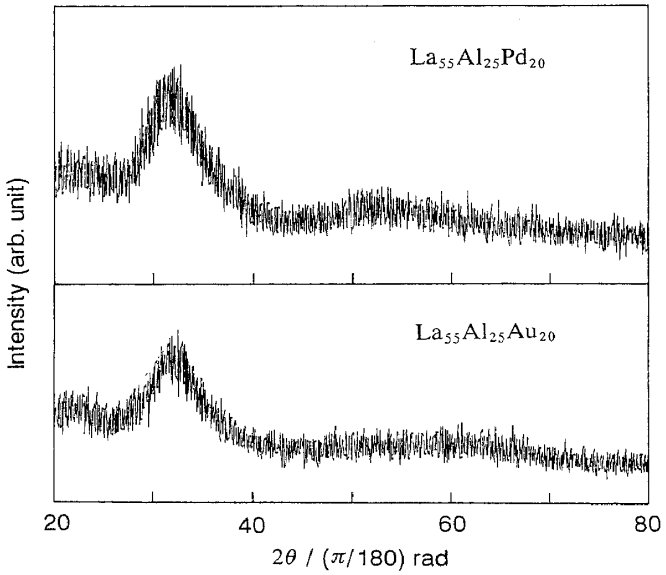

Fig. 16 X-ray diffraction patterns of as-quenched $La_{55}Al_{25}Pd_{20}$ and $La_{55}Al_{25}Au_{20}$ alloy.

on E'(T) and E"(T) at 62.8 rad/s have been presented for the alloy[9]. ΔT_x of the $La_{55}Al_{25}Cu_{20}$ alloy is 54 K, being smaller than that of the $La_{55}Al_{25}Ni_{20}$ alloy. The difference in ΔT_x causes a different E"(T) behavior. In this section, we chose $La_{55}Al_{25}M_{20}$ (M=Ni, Cu, Pd or Au) amorphous alloys to examine the influence of the third element (M) on the glass transition behavior of La-based amorphous alloys.

An amorphous single phase was also found to form in $La_{55}Al_{25}Pd_{20}$ and $La_{55}Al_{25}Au_{20}$ alloys. Figure 16 shows the X-ray diffraction patterns of both the alloys. The patterns consist of only halo peaks and no sharp peak corresponding to a crystalline phase is seen. The atomic ratio of the constituent elements has been pointed out to be one of the important factors for formation of an amorphous phase[14]. Atomic radii of Ni, Cu, Pd and Au[15] are summarized in Table 1, along with the atomic size ratio of these elements to Al. Figure 17 shows T_g, T_x and ΔT_x of the $La_{55}Al_{25}M_{20}$ alloys obtained from the $C_{p,s}(T)$ curves. ΔT_x of the $La_{55}Al_{25}M_{20}$ alloys except M=Pd appears to be dependent on atomic radius. ΔT_x for the $La_{55}Al_{25}Pd_{20}$ alloy is 56 K, which is slightly larger than that (54 K) for the $La_{55}Al_{25}Cu_{20}$ alloy, and the $La_{55}Al_{25}Au_{20}$ alloy has the smallest ΔT_x of 46 K.

Figure 18 shows the temperature dependence of E' and E" in the

Table 1 Atomic radii of Ni, Cu, Pd and Au and the atomic ratios of these elements to Al.

M	Ni	Cu	Pd	Au
r_M/nm	0.125	0.128	0.137	0.144
r_M/r_{Al}	0.874	0.895	0.958	1.01

r_{Al}=0.143nm

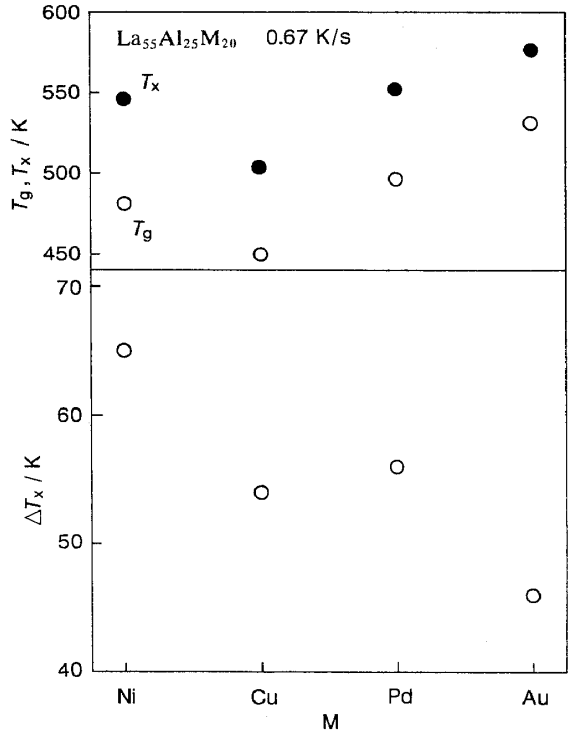

Fig. 17 T_g, T_x and ΔT_x for $La_{55}Al_{25}M_{20}$ (M=Ni, Cu, Pd or Au) amorphous alloys.

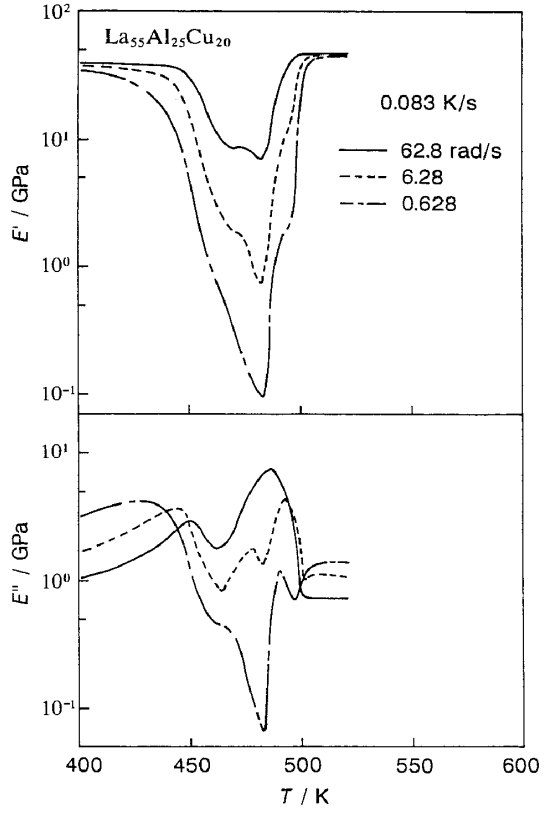

Fig. 18 Change in the temperature dependence of E' and E" for a $La_{55}Al_{25}Cu_{20}$ amorphous alloy.

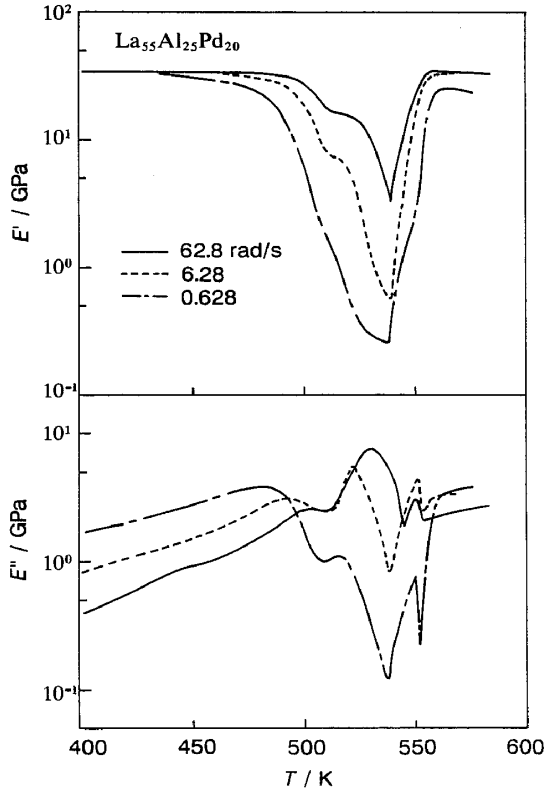

Fig. 19 Change in the temperature dependence of E' and E" for a $La_{55}Al_{25}Pd_{20}$ amorphous alloy.

glass transition region for the $La_{55}Al_{25}Cu_{20}$ alloy measured at different frequencies. The E'(T) curve at 62.8 rad/s shows the two-stage reduction which begins to occur at 446 and 470 K, but the decrease at the second-stage is smaller. On the contrary to the two-stage reduction of E'(T), E"(T) shows peaks at 450 and 487 K. We have presumed that the high-temperature peak at 487 K is due to the incorporation of two peaks due to the second-stage relaxation and the crystallization. As expected, this peak in the case of 62.8 rad/s separates into two peaks with maxima at 477 and 493 K at 6.28 rad/s and two relaxation units are clearly seen on the E"(T) curve. The two relaxation peaks at 446 and 477 K in the case of 6.28 rad/s shift to 429 and 464 K, respectively, at 0.628 rad/s.

Figure 19 shows the temperature dependence of E' and E" in the glass transition region for the $La_{55}Al_{25}Pd_{20}$ alloy measured at different frequencies. E'(T) at 62.8 rad/s indicates the two-stage

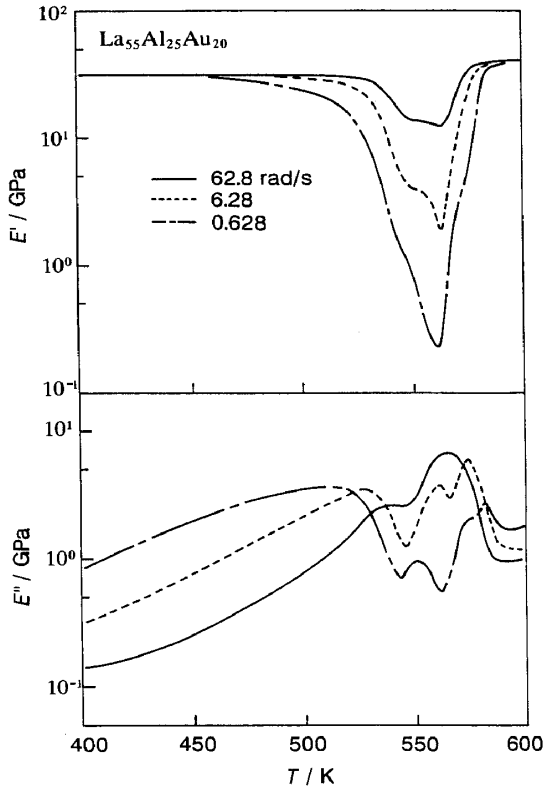

Fig. 20 Change in the temperature dependence of E' and E" for a $La_{55}Al_{25}Au_{20}$ amorphous alloy.

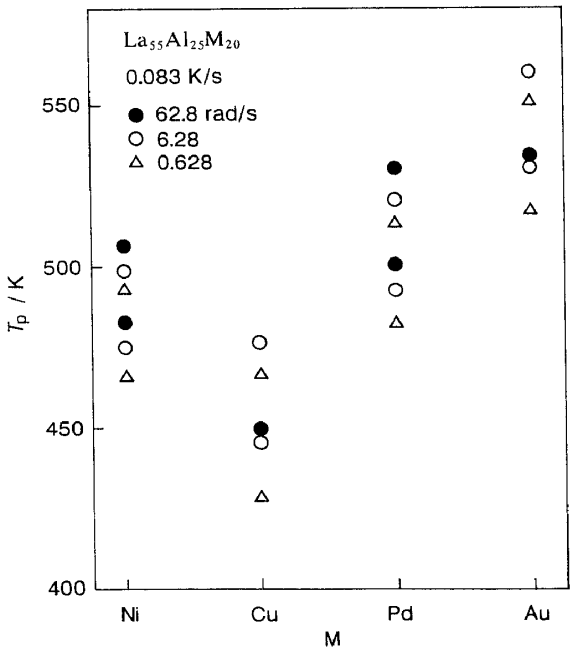

Fig. 21 The peak temperatures of the relaxation peaks in the glass transition region for $La_{55}Al_{25}M_{20}$ (M=Ni, Cu, Pd or Au) amorphous alloys.

reduction which begins to occur at 497 and 511 K. The reduction is more significant in the second stage. E"(T) shows distinctly distinguishable two relaxation peaks at 501 and 531 K and the crystallization peak is seen at 551 K. Although the $La_{55}Al_{25}Pd_{20}$ alloy has a similar ΔT_x value as that for the $La_{55}Al_{25}Cu_{20}$ alloy, the details of the two kinds of relaxation units seem to differ between these alloys. The thermal stability of the supercooled liquid is higher for the $La_{55}Al_{25}Pd_{20}$ alloy than for the $La_{55}Al_{25}Cu_{20}$ alloy. E'(T) and E"(T) behaviors of the $La_{55}Al_{25}Pd_{20}$ alloy are similar to those of the $La_{55}Al_{25}Ni_{20}$ alloy. The similarity is presumably because Ni and Pd belong to the same group with a similar chemical nature. To investigate the influence of the element in the same group as Cu, the temperature dependence of E' and E" in the glass transition region for the $La_{55}Al_{25}Au_{20}$ alloy is shown in Fig. 20. The E'(T) and E"(T) curves is similar to those for the $La_{55}Al_{25}Cu_{20}$ alloy. The similarity is evidenced from the result that the decrease in frequency from

62.8 rad/s causes the separation of the single peak at 546 K to the second-stage relaxation peak and the crystallization peak.

The peak temperatures (T_p) of the relaxations in the glass transition region for the four $La_{55}Al_{25}M_{20}$ (M=Ni, Cu, Pd or Au) alloys are shown in Fig. 21. The lack of the second-stage relaxation peak at 62.8 rad/s is recognized for the M=Cu and Au alloys, suggesting that the mode and process of the relaxations are affected by the chemical nature among the constituent elements. The effect of the atomic radius is clearly recognized in the M elements belonging to the same group of the periodic table. The element which has a larger radius shows a smaller ΔT_x. The valley temperature between two relaxation peaks of E" shown in Figs. 18, 19 and 20 is independent of frequency. The atomic rearrangement affected by the chemical bonding nature among the constituent elements seems to play an important role in the appearance of the two kinds of relaxation units in the glass transition region. The two kinds of relaxation units are also observed in other amorphous alloys with large ΔT_x values such as Zr-[16,17], Mg- and Pd-based alloy systems[18] and the existence of the two kinds of relaxation units seems to be very important in the understanding of the mechanism for the glass transition of amorphous alloys.

IV. Summary

The anelastic relaxation behavior in the temperature regions of sub-T_g and T_g was investigated for $La_{55}Al_{45-x}Ni_x$ (x=0 to 35 %), $La_5Al_{85}Ni_{10}$, and $La_{55}Al_{25}M_{20}$ (M=Cu, Pd and Au) amorphous alloys. These alloys were chosen because a distinct glass transition is observed in wide composition ranges in the La-based alloys. The results obtained are summarized as follows.

(1) The sub-T_g relaxation peak is observed in all the La-Al-Ni ternary alloys. The activation energy for the sub-T_g relaxation is independent of ΔT_x as well as the relaxation behavior at T_g. The sub-T_g relaxation in the La-Al-Ni alloys is mainly due to the local rearrangement of Al-Ni pair.

(2) The relaxation peak at T_g is observed in all the alloys including the $La_{55}Al_{45}$ binary alloy without a distinct endothermic reaction due to T_g in the DSC measurement. Furthermore, the existence of the two kinds of relaxation units near T_g is observed for the $La_{55}Al_{45-x}Ni_x$ alloys in the composition range of x=15 to 30 with ΔT_x exceeding 35 K. The supercooled liquid with higher stability against the

nucleation of a crystalline phase tends to show a more dominant relaxation peak at higher frequencies.

(3) The two kinds of relaxation peaks are also observed for all the $La_{55}Al_{25}M_{20}$ alloys. These relaxation peaks are affected by the chemical nature of the third M element against the other constituent elements. The atomic size ratio of the third M element to the other elements also has a significant influence on the two-stage relaxation behavior.

(4) The existence of the two kinds of glass transition units is important in the understanding of the glass transition behavior of amorphous alloys. The dynamic mechanical measurement which allows the detection of the two kinds of relaxation units in the glass transition region is concluded to be another useful technique as similar to the thermal analytical technique.

Acknowledgment

This work was supported by a Grant-in-Aid for Scientific Research (A) from the Ministry of Education, Science and Culture.

References

(1) H.S. Chen, Rep. Prog. Phys., 43 (1980), 353.

(2) A. Inoue, T. Zhang and T. Masumoto, Mater. Trans., JIM, 30 (1989), 965.

(3) A. Inoue, H. Yamaguchi, T. Zhang and T. Masumoto, Mater. Trans., JIM, 31 (1990), 104.

(4) S. Seki and H. Suga, Kagaku Sosetu, No. 5 (1974), 225.

(5) H. Ino, Amorphous materials, eds. M. Doyama and R. Yamamoto, Tokyo Univ. Pub., Tokyo, (1985), p. 15.

(6) H. Okumura, H.S. Chen, A. Inoue and T. Masumoto, J. Non-Cryst. Solids, in press.

(7) H. Okumura, H.S. Chen, A. Inoue and T. Masumoto, J. Non-Cryst. solids, 130 (1991), 304.

(8) H. Okumura, H.S. Chen, A. Inoue and T. Masumoto, Jpn. J. Appl. Phys., 30 (1991), 2553.

(9) H. Okumura, A. Inoue and T. Masumuto, Mater. Trans., JIM, 32 (1991), 593.

(10) E. Matsubara, Y. Waseda, A. Inoue, K. Ohtera and T. Masumoto, Z. Naturforsch., 44a (1989), 814.

(11) L.C.E. Struik, Physical Aging in Amorphous Polymers and Other Materials, Elsevier, Amsterdam, (1978), p. 115.
(12) H.S. Chen, J. Non-Cryst. Solids, 29 (1978), 223.
(13) Structure and Properties of Polymers, eds. M. Kakudo, H. Kawai and N. Saito, Maruzen, Tokyo, (1963), p. 250.
(14) Materials Sience of Amorphous Metals, ed. T. Masumoto, Ohm Pub., Tokyo, (1982), p.25.
(15) Metals Data book, ed. Jpn. Inst. Metals, Maruzen, Tokyo, (1984), p.8.
(16) H. Okumura, A. Inoue and T. Masumoto, Collected Abstracts of the Annual Meeting of Jpn. Inst. Metals, Sendai, (1990), p. 458.
(17) H. Okumura, A. Inoue and T. Masumoto, Collected Abstracts of the Annual Meeting of Jpn. Inst. Metals, Hiroshima, (1991), p. 504.
(18) H. Okumura, A. Inoue and T. Masumoto, unpublished research, (1990).